Implementation of a DFT-Based Method for the Calculation of the Zeeman *g*-Tensor in Periodic Systems with the Use of Numerical and Slater-Type Atomic Orbitals

Eugene S. Kadantsev* and Tom Ziegler

Department of Chemistry, University of Calgary, Calgary, Alberta, T2N 1N4 Canada

Received: June 20, 2008; Revised Manuscript Received: November 5, 2008

The Zeeman *g*-tensor parameterizes the interaction of an effective electronic spin with the homogeneous external magnetic field in the electron paramagnetic resonance (EPR) experiment. In this article, we describe a Kohn−Sham DFT (KS DFT)-based implementation of the *g* -tensor for periodic systems. Our implementation can be used, for example, for the first-principles calculation of a *g*-tensor of paramagnetic defects in solids. Our approach is based on the method of Van Lenthe et al.[20] in which the spin−orbital coupling is taken into account variationally. The method is implemented in the *BAND* program, a KS DFT implementation for periodic systems. The Bloch states are expanded in the basis of numerical and Slater-type atomic orbitals (NAOs/STOs). Our implementation does not rely on the frozen core approximation tacitly assumed in the pseudopotential schemes. The implementation is validated by calculating the *g*-tensor for small molecules as well as for paramagnetic defects in solids. In particular, we consider ozonide and hydrogen cyanide anion radicals in a KCl host crystal lattice.

I. Introduction

Electron paramagnetic resonance spectroscopy (EPR)[1,2] has become a powerful experimental technique for studing paramagnetic species. Paramagnetic interactions in the EPR experiments are interpreted in terms of an effective EPR Hamiltonian

$$\hat{H}_{\mathrm{EPR}} = \sum_N \mathbf{I}_N A_N \mathbf{S} + \mathbf{S}D\mathbf{S} + \frac{1}{2c}\vec{B}g\mathbf{S} \qquad (1)$$

which contains A_N-, *D*-, and *g*-tensors that parameterize the hyperfine (for nucleus *N*), zero-field splitting, and Zeeman interactions, respectively. In eq 1, the sum is over nuclei with magnetic moment $\mathbf{I}_N$, $\vec{B}$ is the external magnetic field, $\mathbf{S}$ is a spin operator, and *c* is the speed of light (137.03921 in au). Because of the importance of EPR spectroscopy, the first-principles calculation of these EPR tensors is of great interest.

The methods for calculation of the electronic *g*-tensor were reviewed in ref 3. The modern first-principles calculations of the *g*-tensor were pioneered by Lushington and Grain[4−7] in the context of traditional quantum chemistry. The Kohn−Sham density functional theory (KS DFT)[8,9]-based methods for calculation of the *g*-tensor were developed in refs 10 and 11. The methods[4−7,10,11] were developed for isolated molecules only. Many of the EPR experiments are conducted in the crystalline environment, and the molecular approaches for the calculation of the *g*-tensor have to be extended or modified. Pickard and Mauri[12] presented a projector augmented wave (PAW)[13]-based method for calculation of the *g*-tensor under periodic boundary conditions (PBC) and applied their scheme to a phosphorus defect in quartz. A somewhat different approach for the calculation of the *g*-tensor under PBC was presented by Declerck and co-workers in ref 14. The scheme[14] was developed within the framework of first-principles pseudopotentials and a plane wave basis set and was applied to calculate the *g*-tensor of ozonide anion radical in KCl crystal lattice. In both approaches,[12,14] the effects of relativity were treated via perturbation theory.

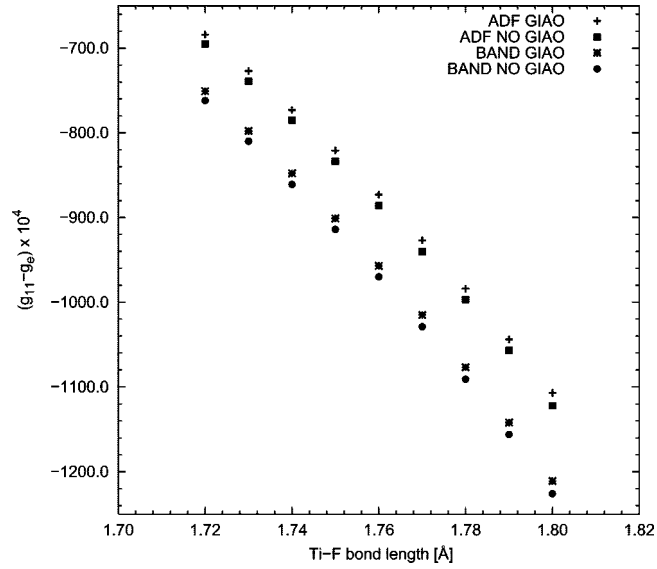

Figure 1. *g*-Tensor shift $\Delta g_{11} = \Delta g_{22}$ in the TiF_3 molecule as a function of the Ti−F bond length in Å. $\Delta g_{ii} = g_{ii} - g_e$. *ADF* and *BAND* two-component LDA calculations with and without GIAO corrections (DZ basis set). The equilibrium Ti−F bond length is 1.78 Å. The *ADF* and *BAND* results differ by a small amount due to the technical differences between the programs. The magnitude and sign of the GIAO corrections is identical in both calculations.

In a previous publication,[15] we have implemented a robust scheme for the calculation of the EPR *A*-tensor of paramagnetic defects in solids. The accurate first-principles calculation of the Zeeman *g*-tensor of paramagnetic defects in solids is the main subject of the present account. In this work, we develop a computational framework that allows one to predict the *g*-tensor based on the KS DFT formalism in conjunction with periodic boundary conditions. In our approach, the paramagnetic defect and its crystalline environment is repeated periodically using supercells that should be large enough to avoid spurious interactions. We make use of a Bloch basis set, which is made

* To whom correspondence should be addresed. E-mail: ekadants@babylon.phy.nrc.ca.

10.1021/jp805466c CCC: $40.75
Published on Web 01/27/2009

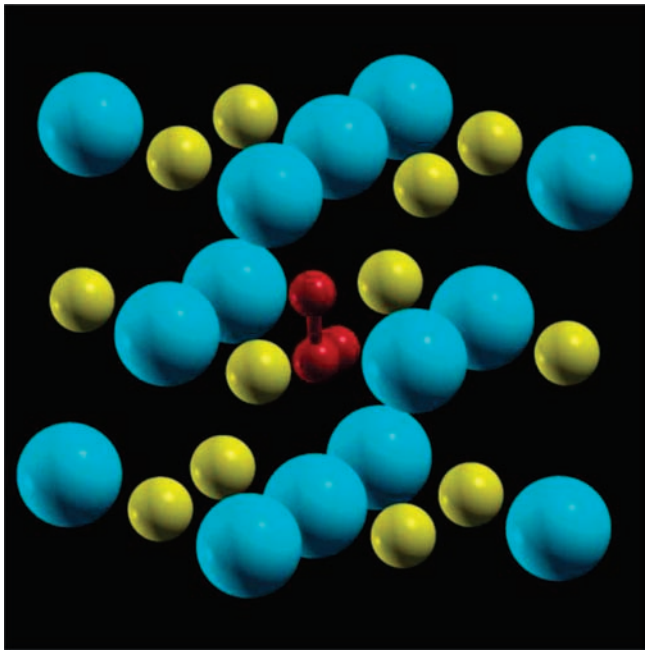

Figure 2. Ozonide anion radical in KCl lattice (cyan, K atoms; yellow, Cl atoms; red, oxygen K atoms).

up of numerical and Slater-type atomic orbitals (NAO/STO Bloch basis). Our approach for the calculation of the *g*-tensor is implemented in the *BAND* program,[16−18] a program for KS DFT calculations on systems with translational invariance. Because localizability is the intrinsic property of the AOs that make up our Bloch basis, it can be computationally advantageous to use a high-quality basis set to describe the paramagnetic defect and treat the rest of the system with a basis of a lower quality. Our implementation does not hinge upon the frozen core approximation;[19] however, the frozen core approximation can be used, in principle, to describe the host core states without compromising the accuracy of the calculation.

We choose to treat the spin−orbital interaction variationally as proposed by van Lenthe et al. in ref 20. In ref 20, the *g*-tensor is computed using degenerate perturbation theory from a pair of two-component spinors (a Kramers doublet) related to each other by time-reversal symmetry. The relativistic effects are included variationally because their treatment based on the perturbation theory is inadequate for heavier elements.[10] The shortcoming of the approach of ref 20 is that spin polarization is neglected; whereas the approaches based on the perturbative treatment of relativity usually include it (for example, the approach).[10] Therefore, the spin-polarized (spin-unrestricted) calculations of the *g*-tensor based on the perturbative treatment of relativistic effects perform better for lighter radicals than the spin-unpolarized (restricted open shell) calculations with variational treatment of spin−orbital coupling. Nevertheless, the spin polarization within the two-component variational treatment of spin−orbital coupling can be included, in principle, in the spirit of refs 21 and 22, and we intend to address the problem of spin polarization in the future. In what follows, we will refer to the approach by van Lenthe et al.[20] and the approaches that treat relativity perturbatively but include spin polarization as 2C/SU (two component/spin unpolarized) and 1C/SP (one component/spin polarized), respectively.

The article is organized as follows. The next section summarizes the derivation of the *g*-tensor within the framework of two-component KS DFT calculations in which the spin−orbital coupling is taken into account variationally. The next section presents results from numerical calculations of the *g*-tensor for localized molecular systems. This is followed by calculations of EPR parameters of paramagnetic defects in solids and the concluding summary. Atomic units $\hbar = e = m_e = 1$ are used throughout unless otherwise specified.

II. Theory

Following van Lenthe et al.,[20] the *g*-tensor is derived by establishing a one-to-one correspondence between the effective EPR Hamiltonian and a microscopic relativistic zero-order regular approximation (ZORA) KS Hamiltonian.[23] In the ZORA approach to relativistic effects, the kinetic energy operator is replaced by the ZORA expression $\hat{T}^{\mathrm{ZORA}}$

$$-\frac{1}{2}p^2 \Rightarrow \hat{T}^{\mathrm{ZORA}} = \vec{\sigma}p\frac{c^2}{2c^2 - V_{\mathrm{SAPA}}(\mathbf{r})}\vec{\sigma}p \tag{2}$$

where p is the momentum operator ($p = -i\nabla$ in the absence of a magnetic field); $V_{\mathrm{SAPA}}(r)$ is a sum of atomic potentials (SAPA), an approximation to the total effective potential in the ZORA kinetic energy operator; and $\vec{\sigma} = \{\sigma_x, \sigma_y, \sigma_z\}$ is a vector made up of the Pauli matrices

$$\sigma_x = \begin{pmatrix} 0 & 1 \\ 1 & 0 \end{pmatrix};\ \sigma_y = \begin{pmatrix} 0 & -i \\ i & 0 \end{pmatrix};\ \sigma_z = \begin{pmatrix} 1 & 0 \\ 0 & -1 \end{pmatrix} \tag{3}$$

Introducing the notation

$$K = \frac{1}{1 - V_{\mathrm{SAPA}}(\mathbf{r})/2c^2} \tag{4}$$

the ZORA kinetic energy becomes

$$\hat{T}^{\mathrm{ZORA}} = \vec{\sigma}p\frac{K}{2}\vec{\sigma}p \tag{5}$$

The nonrelativistic limit can be obtained by setting $K \rightarrow 1$. $\hat{T}^{\mathrm{ZORA}}$ can be split into the so-called scalar relativistic and spin−orbital terms. Using a well-known identity for Pauli matrices

$$(\vec{\sigma}\vec{a})(\vec{\sigma}\vec{b}) = \vec{a}\vec{b} + i\vec{\sigma}(\vec{a} \times \vec{b}) \tag{6}$$

where $\vec{a}$ and $\vec{b}$ are two arbitrary three-component vectors, we obtain

$$\hat{T}^{\mathrm{ZORA}} = \hat{T}^{\mathrm{ZORA}}_{\mathrm{SR}} + \hat{T}^{\mathrm{ZORA}}_{\mathrm{SO}} = p\frac{K}{2}p + \frac{1}{2}\vec{\sigma}(\nabla K \times p) \tag{7}$$

Eq 7 constitutes the ZORA kinetic energy expression in the absence of a magnetic field. The details of ZORA implementation in the BAND program are given in ref 24.

The magnetic field is introduced into the Hamiltonian employing the so-called minimum coupling ansatz[25] in which the momentum operator acting on an electron is modified as $p \rightarrow \Pi = p + \vec{A}/c$ (the negative sign of an electron charge is already taken into account in this expression), where $\vec{A}$ is a vector potential. We then obtain the following chain of equations

$$\hat{T}^{\mathrm{ZORA}} = \vec{\sigma}\Pi\frac{K}{2}\vec{\sigma}\Pi = \Pi\frac{K}{2}\Pi + \frac{i\vec{\sigma}}{2}\left(\left(p + \frac{\vec{A}}{c}\right)K \times \left(p + \frac{\vec{A}}{c}\right)\right) \tag{8}$$

The first term yields

$$\Pi\frac{K}{2}\Pi = p\frac{K}{2}p + \frac{K}{2c}\vec{A}p + p\vec{A}\frac{K}{2c} + \frac{K}{2c^2}\vec{A}^2 \tag{9}$$

whereas the second term is more complicated. We obtain

$$\frac{i\vec{\sigma}}{2}\left(\left(p+\frac{\vec{A}}{c}\right)K\times\left(p+\frac{\vec{A}}{c}\right)\right)$$
$$=\frac{i\vec{\sigma}}{2}(pK\times p)+\frac{i\vec{\sigma}}{2c}(K\vec{A}\times p+p\times\vec{A}\ K)$$
$$=\frac{\vec{\sigma}}{2}(\nabla K\times p)+\frac{\vec{\sigma}}{2c}(\nabla K\times\vec{A})+\frac{K}{2c}\vec{\sigma}\,\vec{B}\cdot\vec{B}=\nabla\times\vec{A} \quad (10)$$

where we used

$$\vec{A}K\times(p\phi)=-(p\phi)\times(\vec{A}K)=\phi p\times(\vec{A}K\phi)-p\times(\vec{A}K\phi),$$
$$p\times(\vec{A}K)=pK\times\vec{A}+K\times p\vec{A} \quad (11)$$

The total expression for the ZORA kinetic energy operator in the presence of the magnetic field is

$$\hat{T}^{\mathrm{ZORA}}=p\frac{K}{2}p+\frac{1}{2}\vec{\sigma}(\nabla K\times p)+\frac{K}{2c}\vec{A}p+p\vec{A}\frac{K}{2c}+\frac{K}{2c^2}\vec{A}^2+$$
$$\frac{K}{2c}\vec{\sigma}\,\vec{B}+\frac{1}{2c}\vec{\sigma}(\nabla K\times\vec{A}) \quad (12)$$

The terms in eq 12 are interpreted in the following way:

• The first and second terms in eq 12

$$p\frac{K}{2}p+\frac{1}{2}\vec{\sigma}(\nabla K\times p)$$

are identified as a scalar relativistic and spin−orbital ZORA terms in the absence of the magnetic field

• The third term in eq 12

$$\frac{K}{2c}\vec{A}p+p\vec{A}\frac{K}{2c}$$

involves a product of momentum operator $p=-i\nabla$ and vector potential $\vec{A}$. In the context of an EPR experiment, this term describes the interaction of a magnetic field (external magnetic field or magnetic field due to nuclear magnetic moments) with the orbital motion of electrons

• The fourth term

$$\frac{K}{2c^2}\vec{A}^2$$

is quadratic in the magnetic field. This term is omitted from consideration for EPR g- and A-tensors as they are linear in the magnetic field. On the other hand, in the theory of NMR shielding this term gives rise to an operator that is bilinear in $\vec{B}$ and a nuclear magnetic moment and is responsible for the diamagnetic shielding. This term is also responsible for the diamagnetic contribution to magnetizabilities as well as for the diamagnetic spin−orbit contributions to indirect spin−spin couplings.

• The last two terms

$$\frac{K}{2c}\vec{\sigma}\vec{B}+\frac{1}{2c}\vec{\sigma}(\nabla K\times\vec{A})$$

couple spin operators and magnetic fields. The terms will be referred to as Zeeman and spin Zeeman terms, respectively. Both terms originate from

$$\frac{i\vec{\sigma}}{2}(\Pi K\times\Pi)$$

The microscopic Hamiltonian that is used to derive the g-tensor can be obtained from eq 12. A homogeneous magnetic field $\vec{B}$ can be obtained from the vector potential of the type

$$\vec{A}(\mathbf{r})=\frac{1}{2}\vec{B}\times\mathbf{r} \quad (13)$$

The vector potential (eq 13) is defined up to a gradient of a scalar function as both $\vec{A}(\mathbf{r})$ and $\vec{A}(\mathbf{r})+\nabla f(\mathbf{r})$ will give rise to the same $\vec{B}$, where $f(\mathbf{r})$ is an arbitrary function.

Introducing a factor $g_e/2$, which is close to unity, the microscopic Hamiltonian H^Z writes

$$H^Z=\frac{g_e}{2c}\left(\frac{K}{2}\vec{\sigma}\vec{B}+\frac{K}{4}\vec{B}\vec{L}+\vec{B}\vec{L}\frac{K}{4}+\vec{\sigma}\left(\nabla\frac{K}{2}\times\vec{A}\right)\right)$$
$$=\frac{g_e}{2c}\left(\frac{K}{2}\vec{\sigma}\vec{B}+\frac{K}{4}\vec{B}\vec{L}+\vec{B}\vec{L}\frac{K}{4}+(\vec{\sigma}\vec{B})\left(\mathbf{r}\nabla\frac{K}{4}\right)-(\vec{\sigma}\mathbf{r})\left(\vec{B}\nabla\frac{K}{4}\right)\right) \quad (14)$$

where $\vec{L}=\mathbf{r}\times p$ is the angular momentum operator.

We assume that the g-tensor is completely determined by a Kramers doublet, which consists of two-component spinors $|\Phi_1\rangle$ and $|\Phi_2\rangle$ related to each other by time-reversal symmetry

$$|\Phi_2\rangle=\{C.C.\}(-i\sigma_y)|\Phi_1\rangle=\{C.C.\}\begin{pmatrix}0&-1\\1&0\end{pmatrix}\begin{pmatrix}\phi_a\\\phi_b\end{pmatrix}=\begin{pmatrix}-\phi_b^*\\\phi_a^*\end{pmatrix} \quad (15)$$

where $\{C.C.\}$ denotes complex cojugation, that is $\{C.C.\}(\mathrm{Re}\ a+i\mathrm{Im}\ a)=(\mathrm{Re}\ a-i\mathrm{Im}\ a)$.

Using degenerate perturbation theory we can write

$$\begin{pmatrix}\langle\Phi_1|H^Z|\Phi_1\rangle&\langle\Phi_1|H^Z|\Phi_2\rangle\\\langle\Phi_2|H^Z|\Phi_1\rangle&\langle\Phi_2|H^Z|\Phi_1\rangle\end{pmatrix}=\frac{1}{2}(\sigma_x(H^Z_{12}+H^Z_{21})+$$
$$\sigma_y(H^Z_{12}-H^Z_{21})+\sigma_z(H^Z_{11}-H^Z_{22}))=\frac{1}{4c}\sum_{lk}\sigma_l g_{kl}B_k \quad (16)$$

where we made use of the fact that any traceless Hermitian 2 × 2 matrix can be expressed as a sum of three Pauli matrices. We determine the elements of the g-tensor g_{kl} from the matrix elements of the type

$$\langle\Phi_i|\frac{\partial H^Z}{\partial B_k}|\Phi_j\rangle \quad (17)$$

where, in our *BAND* implementation,

$$\frac{\partial H^Z}{\partial B_k}=\frac{1}{2c}\frac{g_e}{2}\left(K\sigma_k+\frac{(-i)K}{2}(\mathbf{r}\times\nabla)_k+(\mathbf{r}\times\nabla)_k\frac{(-i)K}{2}\right) \quad (18)$$

In eq 18, we have neglected a small-spin Zeeman contribution.

The individual g-tensor components are given by

$$g_{k1}=4c\frac{\partial}{\partial B_k}\frac{1}{2}(H^Z_{12}+H^Z_{21})=4c\frac{\partial\mathrm{Re}H^Z_{12}}{\partial B_k}=4c\frac{\partial\mathrm{Re}H^Z_{21}}{\partial B_k}$$
$$g_{k2}=4c\frac{\partial}{\partial B_k}\frac{i}{2}(H^Z_{12}-H^Z_{21})=-4c\frac{\partial\mathrm{Im}\,H^Z_{12}}{\partial B_k}=4c\frac{\partial\mathrm{Im}\,H^Z_{21}}{\partial B_k}$$
$$g_{k3}=4c\frac{\partial}{\partial B_k}\frac{1}{2}(H^Z_{11}-H^Z_{22})=4c\frac{\partial\mathrm{Re}H^Z_{11}}{\partial B_k}=-4c\frac{\partial\mathrm{Re}H^Z_{22}}{\partial B_k} \quad (19)$$

Note, that the matrix elements $\langle\Phi_i|\partial H^Z/\partial B_k|\Phi_j\rangle$ determine the g-tensor only in the exact theory, when the spinors are represented using an infinitely large basis set. Because of the

gauge dependence of the vector potential $\vec{A}$, we need to introduce field-depending basis (spinors $\Psi_1(\vec{B})$ and $\Psi_2(\vec{B})$) which coincide, respectively, with Φ_1 and Φ_2 for $\vec{B} = 0$, that is, $\Psi_i(\vec{B} = 0) = \Phi_i$, $i = 1, 2$. If we introduce an explicit dependence of the basis on $\vec{B}$, the g-tensor components will be determined from the matrix elements of the type

$$\left\{\frac{\partial}{\partial B_k}(\langle\Psi_i(\vec{B})|H_{KS}(\vec{B})|\Psi_j(\vec{B})\rangle)\right\}\Big|_{\vec{B}=0} = \langle\Phi_i|\frac{\partial H^Z}{\partial B_k}|\Phi_j\rangle + \langle\frac{\partial\Psi_i(\vec{B})}{\partial B_k}|H^0_{KS}|\Phi_j\rangle + \langle\Phi_i|H^0_{KS}|\frac{\partial\Psi_j(\vec{B})}{\partial B_k}\rangle \quad (20)$$

where H^0_{KS} is the Kohn−Sham Hamiltonian in the absence of the magnetic field.

The two-component eigenstates Φ_1 and Φ_2 of the Hamiltonian H^0_{KS} are already available in the program after the usual self-consistent field procedure, so the first term in eq 20 can be evaluated in a straightforward manner as the expectation value. On the other hand, the field-dependent functions (spinors $\Psi_{i,j}(\vec{B})$) are not available. The field dependence is introduced using the gauge including atomic orbitals (GIAOs) formalism of London and Ditchfield.[26,27] Molecular orbitals (which are two-component spinors) in *BAND* can be written as a linear combination of one-center (two-component) terms, for example,

$$\Phi_1 = \sum_{C,T}\Phi_{1C}(\mathbf{r} - \mathbf{T} - \mathbf{R}_C) \quad (21)$$

where the sum is over atoms C referenced by vectors R_C in the central Wigner−Seitz cell, and, over the lattice vectors $\mathbf{T}$. The one-center term $\Phi_{1C}(\mathbf{r} - \mathbf{T} - \mathbf{R}_C)$ is a linear combination of all of the two-component AOs with common origin at $\mathbf{T} + \mathbf{R}_C$. The coefficients are related to the basis set expansion coefficients and are available in the program. The one-center contributions to the second (time-reversed) spinor Φ_2 can be obtained by time-reversal of individual one-center spinors in eq 21.

To obtain the field-dependence, each of the one-center terms in eq 21 is multiplied by a field-dependent exponential function

$$\tilde{\Phi}_1 = \sum_{C,\mathbf{T}}\Phi_{1C}(\mathbf{r} - \mathbf{T} - \mathbf{R}_C)\exp(-X_C(\mathbf{R}_C, \mathbf{T}))$$

$$X_C(\mathbf{R}_C, \mathbf{T}) = \frac{i}{c}\mathbf{r}\vec{A}(\mathbf{R}_C + \mathbf{T}) = \frac{i}{2c}\vec{B}((\mathbf{R}_C + \mathbf{T}) \times \mathbf{r})$$

$$\tilde{\Phi}_2 = \sum_{D,\mathbf{T}}\Phi_{2D}(\mathbf{r} - \mathbf{T} - \mathbf{R}_D)\exp(-X_D(\mathbf{R}_D, \mathbf{T}))$$

$$X_D(\mathbf{R}_D, \mathbf{T}) = \frac{i}{c}\mathbf{r}\vec{A}(\mathbf{R}_D + \mathbf{T}) = \frac{i}{2c}\vec{B}((\mathbf{R}_D + \mathbf{T}) \times \mathbf{r}) \quad (22)$$

where X depends on the position vector $\mathbf{R}_{C,D} + \mathbf{T}$; $\vec{A}(\mathbf{R}_{C,D} + \mathbf{T})$ is a value of the vector potential $\vec{A}$ at the origin of the one-center term. From $\tilde{\Phi}_1$ and $\tilde{\Phi}_2$, we obtain orthogonal field-dependent spinors by Löwdin orthogonalization to the linear order in field $\vec{B}$

$$(\Psi_1(\vec{B}) \quad \Psi_2(\vec{B})) = (\tilde{\Phi}_1 \quad \tilde{\Phi}_2)\begin{pmatrix}\langle\tilde{\Phi}_1|\tilde{\Phi}_1\rangle & \langle\tilde{\Phi}_1|\tilde{\Phi}_2\rangle\\ \langle\tilde{\Phi}_2|\tilde{\Phi}_1\rangle & \langle\tilde{\Phi}_2|\tilde{\Phi}_2\rangle\end{pmatrix}^{-1/2} \quad (23)$$

where

$$\tilde{\Phi}_i = \Phi_i - \Delta\Phi_i(\vec{B}), \Delta\Phi_i(\vec{B}) = \sum_{C,\mathbf{T}}\Phi_{iC}(\mathbf{r} - \mathbf{R}_C - \mathbf{T})X_C(\mathbf{R}_C, \mathbf{T}) \quad (24)$$

and $\Phi_{iC,T}$ is a short notation for $\Phi_{iC}(\mathbf{r} - \mathbf{R}_C - \mathbf{T})$. For small fields, we can expand the overlap matrix S between $\tilde{\Phi}_i$ and $\tilde{\Phi}_j$ in $\vec{B}$ as

$$(\hat{1} + \Delta S(\vec{B}))^{-1/2} = \hat{1} - \frac{1}{2}\Delta S(\vec{B}) \quad (25)$$

where $\hat{1}$ is a two-by-two identity matrix and elements of matrix $\Delta S(\vec{B})$ are given by

$$\Delta S_{ij}(\vec{B}) = -\langle\Delta\Phi_i(\vec{B})|\Phi_j\rangle - \langle\Phi_i|\Delta\Phi_j(\vec{B})\rangle = -\sum_{C,\mathbf{T}}\langle\Phi_{iC,\mathbf{T}}X_C(\mathbf{R}_C, \mathbf{T})|\Phi_j\rangle - \sum_{D,\mathbf{T}}\langle\Phi_i|X_D(\mathbf{R}_D, \mathbf{T})\Phi_{jD,\mathbf{T}}\rangle \quad (26)$$

The equation for a field-dependent spinor becomes

$$\Psi_i(\vec{B}) = \Phi_i - \Delta\Phi_i(\vec{B}) - 1/2\Delta S_{1i}(\vec{B})\Phi_1 - 1/2\Delta S_{2i}(\vec{B})\Phi_2 \quad (27)$$

and

$$\frac{\partial\Psi_i(\vec{B})}{\partial B_k} = -\frac{\partial\Delta\Phi_i(\vec{B})}{\partial B_k} - 1/2\frac{\partial\Delta S_{1i}(\vec{B})}{\partial B_k}\Phi_1 - 1/2\frac{\partial\Delta S_{2i}(\vec{B})}{\partial B_k}\Phi_2$$

$$\frac{\partial\Delta\Phi_i(\vec{B})}{\partial B_k} = \sum_{C,\mathbf{T}}\langle\Phi_{iC,\mathbf{T}}Y_k(\mathbf{R}_C, \mathbf{T}), Y_k(\mathbf{R}_C, \mathbf{T}) = \frac{i}{2c}((\mathbf{R}_C + \mathbf{T}) \times \mathbf{r})_k$$

$$\frac{\partial\Delta S_{ij}(\vec{B})}{\partial B_k} = T^k_{ij} = -\sum_{C,\mathbf{T}}\langle\Phi_{iC,\mathbf{T}}Y_k(\mathbf{R}_C, \mathbf{T})|\Phi_j\rangle - \sum_{D,\mathbf{T}}\langle\Phi_i|Y_k(\mathbf{R}_D, \mathbf{T})\Phi_{jD,\mathbf{T}}\rangle \quad (28)$$

Taking the latter into account, we obtain, for example,

$$\langle\frac{\partial\Psi_i(\vec{B})}{\partial B_k}|H^0_{KS}|\Phi_j\rangle = -\sum_{C,\mathbf{T}}\langle\Phi_{iC,\mathbf{T}}Y_k(\mathbf{R}_C, \mathbf{T})|H^0_{KS}|\Phi_j\rangle - \frac{1}{2}(T^k_{1i})^\dagger\langle\Phi_1|H^0_{KS}|\Phi_j\rangle - \frac{1}{2}(T^k_{2i})^\dagger\langle\Phi_2|H^0_{KS}|\Phi_j\rangle \quad (29)$$

The full contribution to the g-tensor that stems from the explicit dependence of basis spinors on the magnetic field reads

$$\langle\frac{\partial\Psi_i(\vec{B})}{\partial B_k}|H^0_{KS}|\Phi_j\rangle + \langle\Phi_i|H^0_{KS}|\frac{\partial\Psi_j(\vec{B})}{\partial B_k}\rangle = I_1 + I_2$$

$$I_1 = \frac{i}{2c}(\sum_{C,\mathbf{T}}\langle\Phi_{iC,\mathbf{T}}|((\mathbf{R}_C + \mathbf{T}) \times \mathbf{r})_k V_s|\Phi_j\rangle - \sum_{D,\mathbf{T}'}\langle\Phi_i|((\mathbf{R}_D + \mathbf{T}') \times \mathbf{r})_k V_s|\Phi_{jD,\mathbf{T}'}\rangle)$$

$$+ \frac{i}{2c}(\sum_{C,\mathbf{T}}\langle\Phi_{iC,\mathbf{T}}|((\mathbf{R}_C + \mathbf{T}) \times \mathbf{r})_k\sigma\mathrm{p}\frac{K}{2}\sigma\mathrm{p}|\Phi_j\rangle - \sum_{D,\mathbf{T}'}\langle\Phi_i|\sigma\mathrm{p}\frac{K}{2}\sigma\mathrm{p}((\mathbf{R}_D + \mathbf{T}') \times \mathbf{r})_k|\Phi_{jD,\mathbf{T}'}\rangle)$$

$$I_2 = \frac{Ei}{2c}(-\sum_{C,\mathbf{T}}\langle\Phi_{iC,\mathbf{T}}|((\mathbf{R}_C + \mathbf{T}) \times \mathbf{r})_k|\Phi_j\rangle + \sum_{D,\mathbf{T}'}\langle\Phi_i|((\mathbf{R}_D + \mathbf{T}') \times \mathbf{r})_k|\Phi_{jD,\mathbf{T}'}\rangle) \quad (30)$$

where E is an eigenvalue corresponding to the degenerate spinors $\langle\Phi_i|H^0_{KS}|\Phi_j\rangle = E\delta_{ij}$ and V_s is the Kohn−Sham potential.

TABLE 1: g-Tensor of Small Molecules[a]

molecule	bond length (Å)	g-shift	EXP	1C/SP		2C/SU	
				Declerck et al.	ADF	BAND	ADF
MgF	r(Mg−F) = 1.75	$\Delta g_{\|\|}$	−300	−7	−59	−62	−82
		$\Delta g_{\perp}$	−1300	−1091	−2272	−2047	−2067
AlO	r(Al−O)= 1.62	$\Delta g_{\|\|}$	−900	−59	−139	−268	−322
		$\Delta g_{\perp}$	−2600	3543	−2139	38	85
KrF	r(Kr−F) = 2.15	$\Delta g_{\|\|}$	−2000	−185	−349	−12 478	−11 843
		$\Delta g_{\perp}$	66 000	30 916	52 668	42 437	42 646
TiF_3	r(Ti−F) = 1.78	$\Delta g_{\|\|}$	−11 100		−1604	−2043	−1624
		$\Delta g_{\perp}$	−111 300		−62 735	−109 133	−92 116

[a] $\Delta g_{ii} = g_{ii} - g_e$ in ppm; EXP = experiment (from ref 14); 1C/SP = one-component calculations with spin polarization, relativity is taken into account via perturbation theory; 2C/SU = two-component calculations without spin polarization, spin-orbital coupling is taken into account variationally; *ADF*, *BAND* calculations are performed with *ADF* and *BAND* programs (this work); Declerck et al. results are from ref 14 (plane wave pseudopotential method).

The matrix elements required for the calculation of the g-tensor in *BAND* are computed using eqs 17, 18, and 30. This final expression can also be rewritten to explicitly show gauge independence.[20]

III. Results

A. Small Molecules. The first natural step in testing our implementation for the g-tensor is to perform a calculation on isolated molecular systems in the supercell geometry and to compare results of our approach implemented in the *BAND* program with results obtained with the molecular *ADF* code.[28−30]

We consider several molecules: dimers MgF, AlO, and KrF as well as planar molecule TiF_3 (D_{3h} symmetry). We have carried out one- and two-component calculations in the local density approximation (spin polarized and spin unpolarized) of the g-tensor for these molecules using a large (TZ2P) basis. The main goal of these calculations is not to obtain accurate g-tensor shifts or assess accuracy of density functionals but to verify our *BAND* implementation.

Our results are summarized in Table 1. The g-tensor for these molecular systems has axial symmetry in which two g-tensor components are the same $g_{11} = g_{22} = g_{\perp}$ and the third component $g_{33} = g_{||}$ differs from those two. In agreement with previous observations,[31] it is found that one-component approaches (1C/SP) generally fail to reproduce the $\Delta g_{||} = g_{||} - g_e$ g-shift, whereas two-component approaches (2C/SU) generally fail to reproduce $\Delta g_{\perp} = g_{\perp} - g_e$.

Table 1 shows that *BAND* and *ADF* two-component calculations (the last two columns) are consistent with each other, although there are some discrepancies. For example, there is a discrepancy of about 7% (of the experimental value) in the isotropic shift for TiF_3. More importantly, the differences between *BAND* and *ADF* two-component calculations are much smaller than the differences between these calculations and the experiment. We attribute the difference between *ADF* and *BAND* two-component calculations to several factors. The g-tensor shifts are quite sensitive to the computational details. For example, by examining Table 4 of ref 14 one can see that the results of calculations that are supposed to be on the same "level of theory" (the same exchange-correlation density functional and treatment of relativity) might be quite different. There are also technical differences between *BAND* and *ADF*. *BAND* uses a mixed basis set (NAOs and STOs), whereas basis set in *ADF* is composed of only STOs. The fit functions employed in both programs differ. Therefore, one can never obtain the same numbers with both programs. The absence of spin Zeeman term in our *BAND* implementation as well as supercell effects also contribute to the discrepancy.

We have also tested the GIAO implementation by calculating the g-tensor with a small (DZ) basis with and without GIAO corrections. Figure 1 shows $\Delta g_{11} = \Delta g_{22}$ as a function of the Ti−F bond length. We can see that $\Delta g_{11} = \Delta g_{22}$ becomes more negative as the Ti−F bond length increases. The sign and magnitude of the GIAO corrections are identical in both *ADF* and *BAND* calculations. We find that even for such a small basis, the GIAO corrections are quite small (at least in the case of the TiF_3 molecule).

B. Ozonide O_3^- Anion Radical in KCl Crystal Lattice. The most interesting applications of our approach are those which involve paramagnetic defects in a crystalline environment. As an example, we compute the Zeeman g-tensor of O_3^- in KCl crystal lattice.

With the objective of determining the g-tensor, we first optimize the geometry of O_3^- in the KCl lattice, where the O_3 radical replaces one of the halogen atoms. The constrained geometry optimization is carried out using the VASP code.[32−35] The local spin density approximation (LSDA)[36] is used for the exchange-correlation energy. The PAW formalism[13] is employed as implemented in VASP.[37] The PAW pseudopotentials are taken from the database supplied with VASP, in particular, we use hard pseudopotentials for K, Cl, and O. The LSDA optimized lattice constant for KCl is $a = 6.09$ Å. Three O, 6 nearest K, and 12 Cl atoms were allowed to relax during the constrained geometry optimization. The k-space is sampled using the Γ-point only. The supercell employed in the modeling consists of 8 cubic cells and has 66 atoms in total. In agreement with previous calculations,[14] the ozonide radical is found to lie in the $\{1\bar{1}0\}$ crystal plane (Figure 2). The structure of O_3^- in KCl has C_{2v} symmetry with an oxygen−oxygen bond length of 1.34 Å. The electronic state that corresponds to an unpaired electron is well separated from the valence and conduction bands of KCl and lies approximately 1 eV above the top of the valence band.

The optimized structure for ozonide in the KCl lattice is used in LDA *BAND* Γ-point (two-component) calculations with spin−orbital coupling 2C/SU/S (two-component/spin unpolarized/solid). In our calculations, we use mixed STO/NAO basis sets of TZ2P quality taken from the *BAND* basis set database. To speed up the calculations, we exclude 4f functions from our basis. For K, we also found it necessary to remove one of the 4s functions to avoid linear dependency problems. For oxygen, we use all electron basis. We freeze 1s, 2s, and 2p shells for Cl and K atoms.

To get a better understanding of the effects that influence the g-tensor shifts of O_3^- in KCl, we have also performed two calculations of the g-tensor of O_3^- in vacuum with the molecular

TABLE 2: *g*-Tensor Shifts for Ozonide Anion Radical in a KCl Crystal Lattice and in Vacuum[a]

	KCl crystal lattice			Vacuum	
	EXP	1C/SP Declerck et al.	2C/SU BAND	1C/SP ADF LSDA(GGA)	2C/SU ADF
$g_{iso} - g_e$	0.0088	0.0086	0.0113	0.0098(0.0092)	0.0115
Δg_{11}	0.0009	−0.0005	0.0010	−0.0005(−0.0005)	−0.0004
Δg_{22}	0.0159	0.0168	0.0204	0.0195(0.0182)	0.0231
Δg_{33}	0.0095	0.0094	0.0125	0.0105(0.0099)	0.0119

[a] $g_{iso} = 1/3$ Tr g, $\Delta g_{ii} = g_{ii} - g_e$; EXP, experimental results from ref 38 for ozonide in KCl matrix; 1C/SP, one-component calculations with spin-polarization, relativity is taken into account via perturbation; 2C/SU, two-component calculations without spin-polarization, spin-orbital coupling is taken into account variationally; Declerck et al., plane wave pseudopotential calculation of 1C/SP type for ozonide in KCl matrix (from Ref14); *BAND*, LDA calculation of 2C/SU type for ozonide in KCl matrix with *BAND* PBC program (this work); *ADF*, calculations of 1C/SP and 2C/SU type for ozonide in vacuum with molecular *ADF* program (this work).

TABLE 3: *A*-Tensor for Ozonide Anion Radical in KCl Crystal Lattice and in Vacuum[a]

	KCl crystal lattice		Vacuum
	Declerck etal.	*BAND*	*ADF*
	O_1		
A_{iso}	−69.61	−12.40	−11.90
ΔA_{11}	54.34	39.77	39.58
ΔA_{22}	53.58	37.32	37.41
ΔA_{33}	−107.92	−114.30	−112.68
	O_2		
A_{iso}	−108.65	−24.06	−27.15
ΔA_{11}	71.24	46.01	44.24
ΔA_{22}	74.56	47.64	46.40
ΔA_{33}	−145.81	−165.82	−172.09
	O_3		
A_{iso}	−68.95	−11.55	−11.93
ΔA_{11}	54.17	40.50	39.78
ΔA_{22}	53.39	38.29	37.67
ΔA_{33}	−107.57	−113.43	−113.24

[a] $A_{iso} = 1/3\text{tr}A$, $\Delta A_{ii} = A_{ii} - A_{iso}$; the components of the A-tensor are given in MHz; O_2 is the central oxyen; Declerck et al., plane wave pseudopotential calculation for O_3^- in KCl matrix from ref 14; *BAND*, LSDA nonrelativistic calculation including spin polarization for O_3^- in KCl matrix (this work); *ADF*, LSDA nonrelativistic calculation including spin polarization for O_3^- in vacuum (this work).

TABLE 4: *g*-Tensor Shifts for CNH^- in KCl Crystal Lattice and in Vacuum[a]

	KCl crystal lattice		Vacuum	
	EXP	2C/SU *BAND*	1C/SP *ADF*	2C/SU *ADF*
$g_{iso} - g_e$	−0.002	0.0010	−0.0021	−0.0026
Δg_{11}	0.0012	0.0049	0.0012	0.0010
Δg_{22}	0.0000	0.000	−0.0001	−0.0001
Δg_{33}	−0.0018	−0.0021	−0.0073	−0.0088

[a] $\Delta g_{ii} = g_{ii} - g_e$, $g_{iso} = 1/3$ Trg; EXP, experimental results from ref 40 for CNH^- in KCl matrix; 1C/SP one-component calculations with spin polarization, relativity is taken into account via perturbation; 2C/SU, two-component calculations without spin polarization, spin-orbital coupling is taken into account variationally. *BAND*, LDA calcuation of 2C/SU type for CNH^- in KCl matrix with *BAND*, PBC program (this work); *ADF*, LSDA/*LDA* calculations of 1C/SP and 2C/SU type for CNH^- in vacuum with molecular *ADF* program (this work).

ADF code using local density and generalized gradient approximation (GGA) for exchange-correlation energy. We employ both approaches to the calculation of the g-tensor − the one-component method of Schreckenbach and Ziegler,[10] which is based on the perturbative treatment of relativity but includes spin polarization effects (we refer to it as 1C/SP/V calcultion, one-component/spin-polarized/vacuum), and the two-component method due to van Lenthe et al.,[20] which treats spin−orbital coupling variationally (2C/SU/V, two-component/spin-unpolarized/vacuum). In the molecular calculations, we use the same geometry for O_3^- as that in the calculation with periodic boundary conditions. We employ a basis set of a similar (TZ2P) quality.

The results of our calculations (2C/SU/S, 1C/SP/V, and 2C/SU/V), the experimental results from ref 38, and an earlier plane wave pseudopotential calculation of Declerck et al.[14] under PBC are summarized in Table 2. Declerck et al.[14] treats spin−orbital coupling perturbatively, whereas spin-polarization is included within his approach, we, therefore, will refer to this calculation as 1C/SP/S, one-component/spin-polarized/solid.

We expect that for light radicals such as O_3^-, the inclusion of spin polarization effects is more important that the variational treatment of spin−orbital coupling. As one can see from Table 2, the results of Declerck et al. compare very well with the experiment. It also follows from Table 2 that GGA and LDA exchange-correlation functionals produce very close results for ozonide. We, therefore, will be discussing how the environmental effects influence the g-tensor shifts. Table 2 shows that the largest environmental effect is the reduction of Δg_{22} by 0.0036 from 0.0195 (the spin polarized 1C/SP/V *ADF* calculation in vacuum) to 0.0159 (experiment in KCl crystal lattice). Note that, this reduction is quite large in relative terms as it accounts for, approximately, 23% of the experimental g-tensor shift. Our two-component approach (2C/SU/S) overestimates Δg_{22} (due to the absence of spin polarization effects) but we do obtain a decrease in Δg_{22} by 0.0027 (or by 17% of the experimental g-shift) from 0.0231 (*ADF* two-component calculations in vacuum without spin polarization 2C/SU/V) to 0.0204 (*BAND* two-component calculation 2C/SU/S).

In the case of ozonide, our scheme quantatively describes a reduction of Δg_{22} due to the introduction of the KCl crystalline environment. The magnitude of Δg_{22} is too large in our approach but the relative change in Δg_{22} is well reproduced.

To further investigate the effects of spin polarization, for the same geometry of O_3^- radical in KCl, we have performed a spin polarized nonrelativistic (one-component) calculation and have calculated the hyperfine A-tensor of O_3^- in KCl using eq 14 of ref 15. Our spin-polarized *BAND* calculation in KCl, *ADF* spin-polarized calculations of O_3^- in vacuum, and the plane wave pseudopotential results from ref 14 are summarized in Table 3. Table 3 shows that the enivoronment influences the hyperfine A-tensor of O_3^- in KCl rather weakly. Table 3 also shows that our anisotropic components are in reasonable agreement with those from the plane wave pseudopotential calculations, whereas our isotropic components are smaller by a factor of, approximately, four. One of the possible reasons

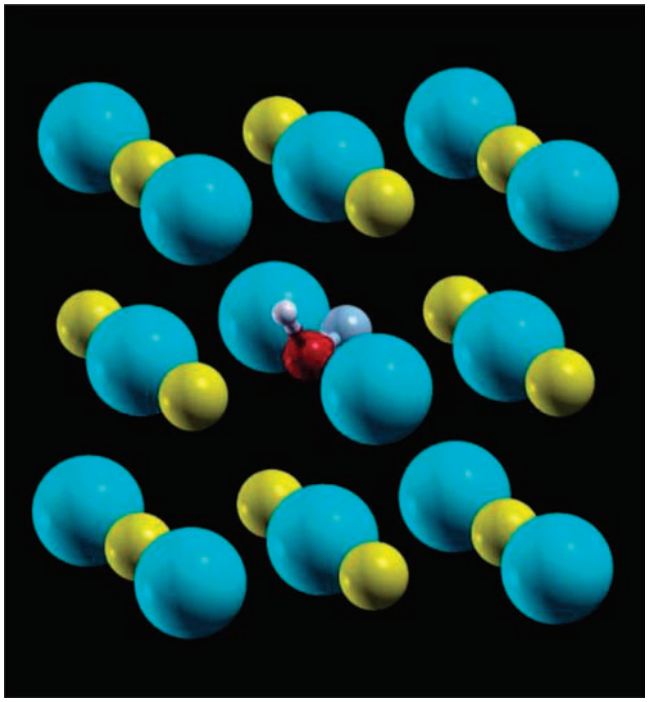

Figure 3. Hydrogen cyanide anion radical in KCl lattice (cyan, K atoms; yellow, Cl atoms; white, a hydrogen; red, carbon atom; gray, nitrogen atom).

for this disagreement is the frozen core approximation assumed in the pseudopotential scheme. We note that the same group have implemented a scheme for calculation of the hyperfine parameters which does not rely on the frozen core approximation[39] but this scheme, to our knowledge, was not applied to the calculation of O_3^- in KCl.

C. Hydrogen Cyanide CNH^- Anion Radical in KCl Crystal Lattice. We have also determined the g-tensor components of the hydrogen cyanide anion radical in a KCl crystal lattice. Experimental results are taken from ref 40. The procedure for determination of g-tensor components of CNH^- in KCl follows that of ozonide. We first performed VASP geometry optimization. As in the case of ozonide, we use 66 atom supercell in which hydrogen cyanide replaces one of the Cl atoms. The radical is found to lie in the $\{1\bar{1}0\}$ crystal plane. The geometry optimization is followed by a two-component BAND LDA calculations with accurate (TZ2P) basis. We have also performed 2C/SU and 1C/SP calculations on the g-tensor in vacuum using the molecular *ADF* code. The results of these calculations and the experiment are summarized in Table 4.

Table 4 shows that the largest g-shifts are Δg_{11} and Δg_{33}. Neither of the theoretical methods employed were able to reproduce both g-shifts. *ADF* results in vacuum agree reasonably well with the experimental Δg_{11} value; however, the Δg_{33} shift as obtained in *ADF* vacuum calculations is too negative. On the other hand, our *BAND* calculations in KCl crystal lattice reduce the negativity of the Δg_{33} g-shift from -0.0088 (2C/SU/V) to -0.0021, and agree with the experimental Δg_{33} g-shift well. The isotropic g_{iso} is overestimated in the *BAND* calculations, whereas it is too small in the *ADF* calculations. The reasons for the discrepancy between theory and experiment may stem from the shortcomings of LDA. We also note that we have previously encountered difficulties in the calculation of hyperfine parameters for this system—it was found that hyperfine parameters for carbon were well reproduced, whereas there were discrepancies in anisotropic A-tensor components for nitrogen.[15]

III. Conclusions

We have developed a Kohn−Sham DFT (KS DFT)-based approach for the calculation of g-tensors in periodic systems. The required equations were implemented in the *BAND* program, a KS DFT implementation for systems with translational invariance which directly make use of a Bloch basis set made up of Slater-type and numeric atomic orbitals.

Our approach is based on the method of Van Lenthe et al.[20] in which the spin−orbital coupling is taken into account variationally and the g-tensor is calculated in the basis of two spinors related to each other by time-reversal symmetry. The shortcoming of this approach is that the effects due to spin polarization are neglected. These effects can be included, in principle, via noncollinear formalism of DFT[41,42] in the spirit of refs 21 and 22 and we plan to address this problem in the future.

Our implementation has been validated by calculating the g-tensor for small molecules as well as for paramagnetic defects in solids. In particular, we consider ozonide and hydrogen cyanide anion radicals in a KCl host crystal lattice. In the case of ozonide anion radical, our two-component implementation reproduces the main environmental effect—a decrease in the Δg_{22} g-shift. Whereas the magnitude of the Δg_{22} g-shift is too large in our approach, the relative change in the Δg_{22} g-shift due to the placement of a radical in the crystalline environment is well reproduced. The discrepancy between theory and experiment for this system is likely due to the absence of spin polarization effects. In the case of the hydrogen cyanide anion radical, our *BAND* calculations reproduce the experimental Δg_{33} g-shift, whereas Δg_{11} is too large compared to the experiment. LDA shortcomings might play a role in the discrepancy between theory and experiment for this system.

Acknowledgment. E.K. acknowledges financial support from the Alberta Ingenuity Fund and stimulating discussions with Dr. P. H. T. Philipsen.

References and Notes

(1) Zavoisky, E. K. *J. Phys. USSR* **1945**, *9*, 221.
(2) Abragam, A.; Bleany, B. *Electron Paramagnetic Resonance of Transition Ions*; Clarendon Press: Oxford, 1970.
(3) *Calculation of NMR and EPR Parameters. Theory and Applications*; Kaupp, M., Bühl, M., Malkin, V. G. Eds.; Wiley-VCH: New York, 2004.
(4) Lushington, G. H.; Bündgen, P.; Grein, F. *Int. J. Quantum Chem.* **1995**, *55*, 377.
(5) Lushington, G. H.; Grein, F. *Int. J. Quantum Chem.* **1996**, *60*, 467.
(6) Lushington, G. H.; Grein, F. *Theor. Chim. Acta* **1996**, *93*, 259.
(7) Lushington, G. H.; Grein, F. *J. Chem. Phys.* **1997**, *106*, 3292.
(8) Hohenberg, P.; Kohn, W. *Phys. Rev.* **1964**, *136*, B864.
(9) Kohn, W.; Sham, L. J. *Phys. Rev.* **1965**, *140*, A1133.
(10) Schreckenbach, G.; Ziegler, T. *J. Phys. Chem. A* **1997**, *101*, 3388.
(11) Patchkovskii, S.; Ziegler, T. *J. Phys. Chem. A* **2001**, *105*, 5490.
(12) Pickard, C. J.; Mauri, F. *Phys. Rev. Lett.* **2002**, *88*, 086403.
(13) Blöchl, P. E. *Phys. Rev.* **1994**, *50*, 17953.
(14) Declerck, R.; Van Speybroeck, V.; Waroquier, M. *Phys. Rev. B* **2006**, *73*, 115113.
(15) Kadantsev, E. S.; Ziegler, T. *J. Phys. Chem. A* **2008**, *112*, 4521.
(16) te Velde, G.; Baerends, E. J. *Phys. Rev. B* **1991**, *44*, 7888.
(17) Wiesenekker, G.; Baerends, E. J. *J. Phys.: Condens. Matter* **1991**, *3*, 6721.
(18) te Velde, G.; Baerends, E. J.; Philipsen, P. H. T.; Wiesenekker, G.; Groeneveld, J. A.; Berger, J. A.; de Boeij, P. L.; Klooster, R.; Kootstra, F.; Romaniello, P.; Snijders, J. G.; Kadantsev, E. S.; Ziegler, T. BAND 2007.01. *SCM: Theoretical Chemistry*, Vrije Universiteit: Amsterdam, The Netherlands.
(19) von Barth, U.; Gelatt, C. D. *Phys. Rev. B* **1980**, *21*, 22.
(20) van Lenthe, E.; Wormer, P. E. S.; van der Avoird, A. *J. Chem. Phys.* **1997**, *107*, 2488.
(21) Jayatilaka, D. *J. Chem. Phys.* **1998**, *108*, 7587.
(22) Malkin, I.; Malkina, O. L.; Malkin, V. G.; Kaupp, M. *J. Chem. Phys.* **2005**, *123*, 244103.

(23) van Lenthe, E.; Snijders, J. G.; Baerends, E. J. *J. Chem. Phys.* **1996**, *105*, 6505.
(24) Philipsen, P. H. T.; van Lenthe, E.; Baerends, E. J. *Phys. Rev. B* **1997**, *56*, 13556.
(25) McWeeny, R. *Methods of Molecular Quantum Mechanics*; Academic Press: San Diego, 1992; p 359.
(26) London, F. *J. Phys. Radium* **1937**, *8*, 397.
(27) Ditchfield, R. *Mol. Phys.* **1974**, *27*, 789.
(28) Baerends, E. J.; Autschbach, J.; Bérces, A.; Bickelhaupt, F. M.; Bo, C.; Boerrigter, P. M.; Cavallo, L.; Chong, D. P.; Deng, L.; Dickson, R. M.; Ellis, D. E.; van Faassen, M.; Fan, L.; Fischer, T. H.; Fonseca Guerra, C.; van Gisbergen, S. J. A.; Groeneveld, J. A.; Gritsenko, O. V.; Grüning, M., Harris, F. E., van den Hoek, P.; Jacob, C. R.; Jacobsen, H.; Jensen, L.; van Kessel, G.; Kootstra, F.; van Lenthe, E.; McCormack, D. A.; Michalak, A.; Neugebauer, J.; Nicu, V. P.; Osinga, V. P.; Patchkovskii, S.; Philipsen, P. H. T.; Post, D.; Pye, C. C.; Ravenek, W.; Ros, P.; Schipper, P. R. T.; Schreckenbach, G.; Snijders, J. G.; S'ola, M.; Swart, M.; Swerhone, D.; te Velde, G.; Vernooijs, P.; Versluis, L.; Visscher, L.; Visser, O.; Wang, F.; Wesolowski, T. A.; van Wezenbeek, E. M.; Wiesenekker, G.; Wolff, S. K.; Woo, T. K.; Yakovlev, A. L.; Ziegler, T. ADF 2007.01. *SCM: Theoretical Chemistry*; Vrije Universiteit, Amsterdam, The Netherlands.
(29) te Velde, G.; Bickelhaupt, F. M.; van Gisbergen, S. J. A.; Fonseca Guerra, C.; Baerends, E. J.; Snijders, J. G.; Ziegler, T. *J. Comput. Chem.* **2001**, *22*, 931.
(30) Fonseca Guerra, C.; Snijders, J. G.; te Velde, G.; Baerends, E. J. *Theor. Chem. Acc.* **1998**, *99*, 391.
(31) Patchkovskii, S.; Schreckenbach, G. *Calculation of NMR and EPR Parameters*, *Theory and Applications*; *Chap. 32*, pp 505−531.
(32) Kresse, G.; Hafner, J. *Phys. Rev. B* **1993**, *47*, 558.
(33) Kresse, G.; Hafner, J. *Phys. Rev. B* **1994**, *49*, 14251.
(34) Kresse, G.; Furthmüller, J. *Comput. Mater. Sci.* **1996**, *6*, 15.
(35) Kresse, G.; Furthmüller, J. *Phys. Rev. B* **1996**, *54*, 11169.
(36) von Barth, U.; Hedin, L. *J. Phys. C: Solid State Phys.* **1972**, *5*, 1629.
(37) Kresse, G.; Joubert, D. *Phys. Rev. B* **1999**, *59*, 1758.
(38) Callens, F.; Matthys, P.; Boesman, E. *J. Phys. C: Solid State Phys.* **1988**, *21*, 3159.
(39) Declerck, R.; Pauwels, E.; Van Speybroeck, V.; Waroquier, M. *Phys. Rev. B* **2006**, *74*, 245103.
(40) Adrian, F. J.; Cochran, E. L.; Bowers, V. A.; Weatherley, B. C. *Phys. Rev.* **1969**, *177*, 129.
(41) Sandratskii, L. M.; Guletskii, P. G. *J. Phys. F: Met. Phys.* **1986**, *16*, L43.
(42) Kübler, J.; Höck, K. H.; Sticht, J.; Williams, A. R. *J. Phys. F: Met. Phys.* **1988**, *18*, 469.
(43) DeVore, T. C., Jr *J. Am. Chem. Soc.* **1977**, *99*, 4700.

JP805466C